Dalton Transactions

ROYAL SOCIETY OF CHEMISTRY

PAPER

View Article Online
View Journal | View Issue

Cite this: *Dalton Trans.*, 2021, **50**, 11472

Mechanochemical synthesis and structural analysis of trivalent lanthanide and uranium diphenylphosphinodiboranates†

Taylor V. Fetrow and Scott R. Daly *

Phosphinodiboranates ($H_3BPR_2BH_3^-$) are a class of borohydrides that have merited a reputation as weakly coordinating anions, which is attributed in part to the dearth of coordination complexes known with transition metals, lanthanides, and actinides. We recently reported how $K(H_3BP^tBu_2BH_3)$ exhibits sluggish salt elimination reactivity with f-metal halides in organic solvents such as Et_2O and THF. Here we report how this reactivity appears to be further attenuated in solution when the ^{t}Bu groups attached to phosphorus are exchanged for R = Ph or H, and we describe how mechanochemistry was used to overcome limited solution reactivity with $K(H_3BPPh_2BH_3)$. Grinding three equivalents of $K(H_3BPPh_2BH_3)$ with $UI_3(THF)_4$ or LnI_3 (Ln = Ce, Pr, Nd) allowed homoleptic complexes with the empirical formulas $U(H_3BPPh_2BH_3)_3$ (**1**), $Ce(H_3BPPh_2BH_3)_3$ (**2**), $Pr(H_3BPPh_2BH_3)_3$ (**3**), and $Nd(H_3BPPh_2BH_3)_3$ (**4**) to be prepared and subsequently crystallized in good yields (50–80%). Single-crystal XRD studies revealed that all four complexes exist as dimers or coordination polymers in the solid-state, whereas ^{1}H and ^{11}B NMR spectra showed that they exist as a mixture of monomers and dimers in solution. Treating **4** with THF breaks up the dimer to yield the monomeric complex $Nd(H_3BPPh_2BH_3)_3(THF)_3$ (**4-THF**). XRD studies revealed that **4-THF** has one chelating and two dangling $H_3BPPh_2BH_3^-$ ligands bound to the metal to accommodate binding of THF. In contrast to the results with $K(H_3BPPh_2BH_3)$, attempting the same mechanochemical reactions with $Na(H_3BPH_2BH_3)$ containing the simplest phosphinodiboranate were unsuccessful; only the partial metathesis product $U(H_3BPH_2BH_3)I_2(THF)_3$ (**5**) was isolated in poor yields. Despite these limitations, our results offer new examples showing how mechanochemistry can be used to rapidly synthesize molecular coordination complexes that are otherwise difficult to prepare using more traditional solution methods.

Received 12th June 2021,
Accepted 16th July 2021

DOI: 10.1039/d1dt01932e

rsc.li/dalton

Introduction

Mechanochemistry,[1–10] defined as a chemical reaction induced by absorption of mechanical energy,[11,12] has been used to synthesize coordination complexes and organic chemicals,[13–24] materials,[25–32] and pharmaceuticals.[33,34] The principle advantages of mechanochemistry are that it requires little to no solvent (which can lead to "greener" chemical processes)[35,36] and it has proven useful for the synthesis of complexes that cannot be prepared using more conventional solution methods.

Although mechanochemistry has seen a resurgence in popularity in recent years,[8] it has long been used to prepare metal borohydride complexes, including those with f-elements.[37,38] For example, in 1976 Volkov and Myakishev reported that $U(BH_4)_4$ can be prepared by ball milling UCl_4 with $LiBH_4$.[39] More contemporary mechanochemical examples include the synthesis of lanthanide tetrahydroborate salts[40,41] and highly volatile lanthanide complexes containing chelating borohydrides called aminodiboranates.[42,43] Mechanochemistry has also been used to synthesize organometallic scandium and lanthanide complexes that are difficult to prepare by solution routes.[44–46]

Recently we described how mechanochemistry could be used to improve upon the poor and inconsistent solution yields of a new class of homoleptic phosphinodiboranate complexes with the empirical formula $M(H_3BP^tBu_2BH_3)_3$ where M = lanthanide or uranium.[47,48] In general, phosphinodiboranates are monoanionic borohydride ligands that can be described as two BH_3 groups joined by a phosphido linker (Chart 1), and they are P congeners of the aforementioned aminodiboranates.[42,43,49–54] Phosphinodiboranates have been known for over 50 years with a wide range of different R substituents attached to phosphorus.[55–77] However, aside from our

Department of Chemistry, The University of Iowa, E331 Chemistry Building, Iowa City, Iowa 52242, USA. E-mail: scott-daly@uiowa.edu

† Electronic supplementary information (ESI) available. CCDC 2089074–2089078, 2089081 and 2089083. For ESI and crystallographic data in CIF or other electronic format see DOI: 10.1039/d1dt01932e

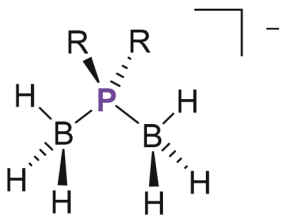

Chart 1 Phosphinodiboranate anions ^{t}Bu-PDB (R = ^{t}Bu), Ph-PDB (R = Ph), and H-PDB (R = H).

previous work with $H_3BP^tBu_2BH_3^-$ (^{t}Bu-PDB),[47,48] there are few examples of phosphinodiboranate complexes beyond those that have been reported with alkali and alkaline earth metals.[63,78,79]

Building on our previous effort with ^{t}Bu-PDB, we began to explore the synthesis of lanthanide and actinide complexes with $H_3BPPh_2BH_3^-$ (Ph-PDB) and the unsubstituted phosphinodiboranate $H_3BPH_2BH_3^-$ (H-PDB). These anions have Ph and H substituents that are less electron donating than the alkyl substituents in ^{t}Bu-PDB, and they are presumed to be more weakly coordinating as a result. Only a few structurally characterized metal Ph-PDB complexes have been reported to date: an Fe(II) complex with a non-coordinating, outer-sphere Ph-PDB to balance the charge,[78] a potassium salt with 18-crown-6,[80] and very recently a heteroleptic magnesium complex prepared *in situ* by Manners and co-workers.[79] In contrast, we are not aware of any metal complexes that have been structurally characterized with H-PDB. Moreover, H-PDB has been exploited for the development of new ionic liquids, apparently because it is so weakly coordinating.[81]

Here we report the mechanochemical synthesis of homoleptic $M(H_3BPPh_2BH_3)_3$ complexes with M = U (**1**), Ce (**2**), Pr (**3**), and Nd (**4**). Using the synthesis of **4** as a representative case study, we compare mechanochemical and solution salt metathesis reactions using different solvents and conditions and we describe the reaction of **4** with THF. Finally, we discuss our attempts to prepare H-PDB complexes using similar means along with the structure of $U(H_3BPH_2BH_3)I_2(THF)_3$ (**5**).

Results and discussion

Synthesis of Ph-PDB complexes

The uranium Ph-PDB complex $U(H_3BPPh_2BH_3)_3$ (**1**) was prepared by grinding three equiv. of $K(H_3BPPh_2BH_3)$ and $UI_3(THF)_4$ at 1800 rpm for 90 min using stainless steel balls (eqn (1), Scheme 1). The lanthanide complexes **2–4** were prepared similarly using base-free MI_3 where M = Ce, Pr, and Nd (eqn (2), Scheme 1). Liquid assisted grinding (LAG)[82] methods were used to prepare all the complexes by adding several drops of Et_2O to the ball mill jars prior to the milling process. The resulting Ph-PDB complexes were separated from the generated KI salt and unreacted starting material by extraction with chlorobenzene or fluorobenzene. All four complexes were crystallized from DCM and Et_2O and isolated in good yields (50–80%).

Attempts to prepare **1–4** by mixing the same reagents in THF and Et_2O yielded no evidence of reactivity. To better quantify the influence of different solvents on product formation for comparison to our ball milling reactions, we used ^{11}B NMR spectroscopy to investigate reaction mixtures containing three equiv. of $K(H_3BPPh_2BH_3)$ and NdI_3 in THF, Et_2O, and chlorobenzene. Data were collected after allowing the mixtures to stir at RT for 24 h.

No ^{11}B resonances consistent with the formation of $Nd(H_3BPPh_2BH_3)_3$ (**4**) or its Lewis base adducts were observed when the reactions were conducted in THF and Et_2O. Only a large peak assigned to the THF-soluble $K(H_3BPPh_2BH_3)$ starting material appeared at δ −34.6 ppm in THF (Fig. S2; ESI†). Similarly, no ^{11}B resonances were detected when the same

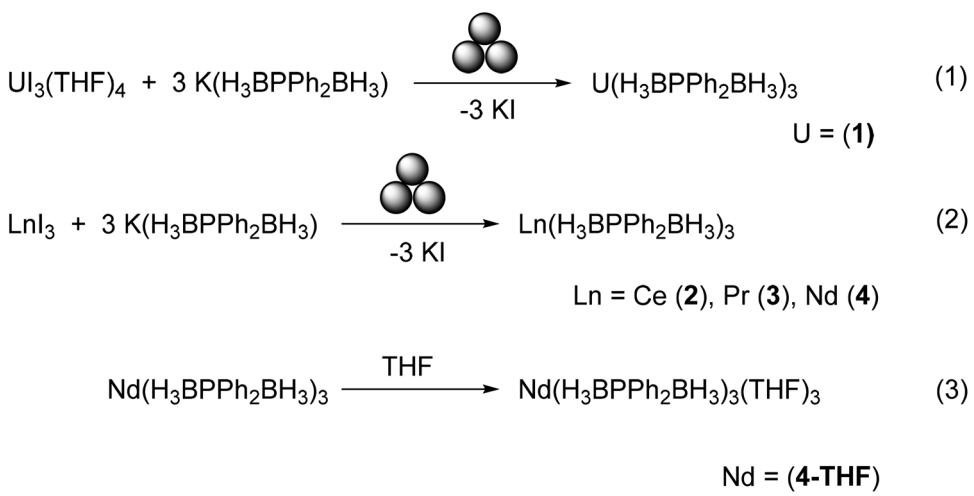

Scheme 1 Mechanochemical synthesis of **1–4** and a subsequent conversion of **4** to **4-THF**. The three circles arranged in a triangle are used to indicate ball milling.[16]

reactions were conducted in Et_2O, even for $K(H_3BPPh_2BH_3)$, which is effectively insoluble in this solvent. Relevant to the discussion of solubility, we note that the metal iodide starting materials form etherate adducts in THF and Et_2O that are at least semi-soluble in their corresponding solvents. For example, La Pierre and coworkers reported that the solubility of $NdI_3(Et_2O)_3$ in Et_2O is 29.1 mM based on UV-vis measurements.[83]

We next tried chlorobenzene, which was selected for comparison because Edelstein and coworkers showed that this solvent could be used to prepare base-free $M(MeBH_3)_4$ where M = Zr, Th, U, and Np by treating the corresponding MCl_4 with 4 equiv. of $Li(MeBH_3)$.[84] In contrast to the reactions conducted in THF and Et_2O, stirring three equiv. of $K(H_3BPPh_2BH_3)$ and NdI_3 in chlorobenzene for 24 h at RT yielded a small ^{11}B NMR resonance at δ 95.3 ppm consistent with the formation of **4** (Fig. 1). Increasing the starting temperature to 50 °C yielded slightly more **4**, but also revealed evidence of decomposition. Performing the reaction at 100 °C yielded no evidence of **4**; only resonances attributed to decomposition were observed.

To compare the solution results side-by-side with our mechanochemical results, we ball milled NdI_3 with three equiv. of $K(H_3BPPh_2BH_3)_3$ at 1800 rpm for 90 min at the same scale as our reactions using organic solvents. The residue was then extracted with the same volume of chlorobenzene used in our solvent study (Fig. 1). Analysis of the extract by ^{11}B NMR spectroscopy showed a higher concentration of **4** based on the increased intensity of the resonance at δ 95.3 ppm as well as the appearance of two new features at δ 75.6 and 176.5 ppm. These are the same ^{11}B resonances observed when analytically pure crystals of **4** are dissolved in chlorobenzene (the assignment of these three resonances will be described below). These results demonstrate how the mechanochemical reactions are higher yielding and faster than comparable reactions performed in solution.

XRD studies of homoleptic Ph-PDB complexes

Single-crystal X-ray diffraction (XRD) studies were carried out to investigate the structures of **1–4**. Two types of crystals with slightly different morphologies were observed for **1**, and XRD studies revealed these to be different structural isomers. The first structure, which is designated as **1a** (Chart 2), is a coordination polymer with each uranium coordinated to one chelating Ph-PDB and four bridging Ph-PDB ligands that link together adjacent uranium ions in the unit cell (Fig. 2). The geometry around U is distorted octahedral based on the arrangement of the six boron atoms with the largest B–U–B angles being 147.0(2)°, 165.5(2)°, and 173.8(2)°. The second structural isomer of $U(H_3BPPh_2BH_3)_3$ (**1b**) is a dimer similar to the structure reported previously for the ^{t}Bu-PDB complex $U(H_3BP^tBu_2BH_3)_3$. The geometry around U in **1b** is distorted trigonal prismatic based again on the arrangement of boron atoms and as indicated by the more acute B–U–B angles of 137.4(6)°, 143.9(2)°, and 154.3(7)° compared to those in **1a**.

The structure of $Ce(H_3BPPh_2BH_3)_3$ (**2**) with the largest lanthanide in our series is identical to polymeric **1a** (Fig. 3) with one chelating Ph-PDB and four Ph-PDB ligands bridging to adjacent cerium ions, whereas the structures of $Pr(H_3BPPh_2BH_3)_3$ (**3**) and $Nd(H_3BPPh_2BH_3)_3$ (**4**) are both dimers like **1b**. Both **3** and **4** crystallize in the monoclinic space group $P2_1/c$ but subtle differences are observed in the two structures presumably due to the differences in ionic radii for Pr^{3+} (0.99 Å) and Nd^{3+} (0.983 Å).[85] The structure of **4** contains a

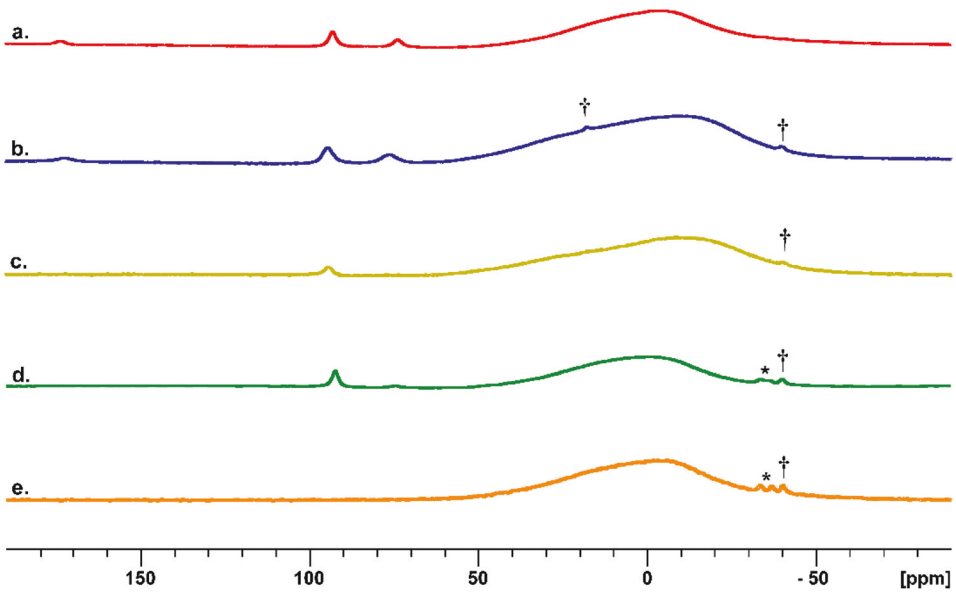

Fig. 1 ^{11}B NMR spectra of (a) crystalline $Nd(H_3BPPh_2BH_3)_3$ (**4**) dissolved in chlorobenzene; (b) chlorobenzene extract (20 mL) from ball-milled reaction mixture of NdI_3 with three equiv. of $K(H_3BPPh_2BH_3)$; (c) mixture of NdI_3 and three equiv. of $K(H_3BPPh_2BH_3)$ stirred in 20 mL of chlorobenzene for 24 h at RT; (d) same mixture as c stirred for 24 h at 50 °C; (e) same mixture as c stirred for 24 h at 100 °C. The * is assigned to decomposition products generated at elevated temperatures. The † is assigned to small amounts of hydrolysis or starting material. The large broad feature centered around δ 0 ppm is attributed to borosilicate inside the instrument.

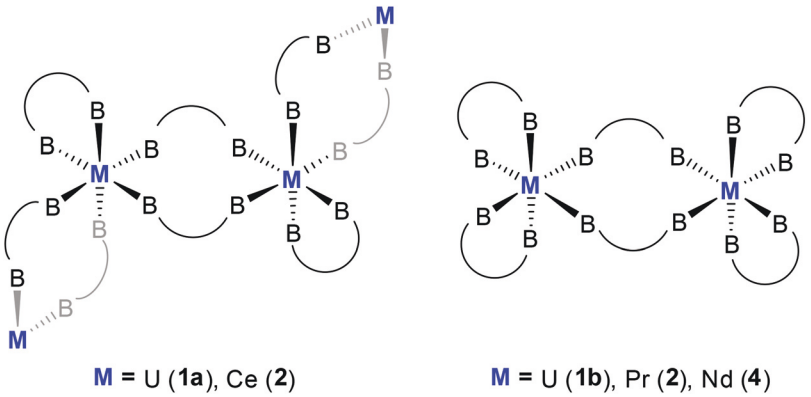

Chart 2 Simplified structural framework of **1–4**. B–B = $H_3BPPh_2BH_3^-$.

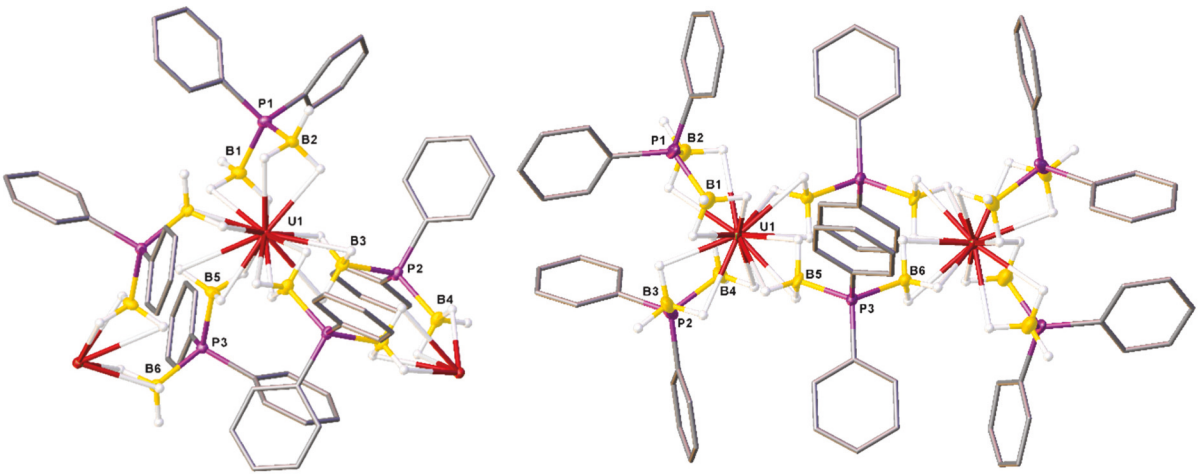

Fig. 2 Structural isomers **1a** (left) and **1b** (right) of $U(H_3BPPh_2BH_3)_3$. Ellipsoids shown at 35% probability. The phenyl rings are represented as pipes and hydrogens attached to carbon are omitted for clarity.

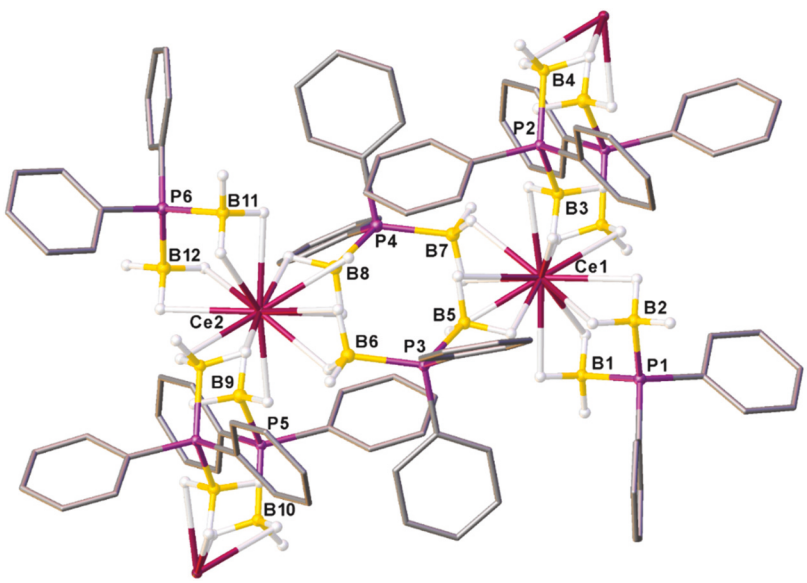

Fig. 3 Molecular structure of $Ce(H_3BPPh_2BH_3)_3$ (**2**). Ellipsoids shown at 35% probability. The phenyl rings are represented as pipes and all hydrogens attached to carbon are omitted for clarity.

mirror plane so that half of the dimer represents the smallest asymmetric unit (one metal, one bridging Ph-PDB, and two chelating Ph-PDB ligands) (Fig. 4). The mirror plane is lost as the metal ion size increases in **3** so that all atoms in the dimer are symmetrically inequivalent.

Given the difficulties accurately assigning the position of hydrogen atoms using single-crystal XRD, metal–boron bond distances are often used to estimate the denticity of borohydride ligands and determine the overall metal coordination number.[86] To facilitate this analysis and show how the M–B bond distances change as a function of metal and structure type (polymer *vs.* dimer), we plotted the M–B distances as a function of the ionic radii of the metal (Fig. 5). Plotting the M–B bond distances this way reveals clustering indicative of the different BH_3 coordination modes (κ^1, κ^2, or κ^3; Chart 3). Starting with the structural isomers of $U(H_3BPPh_2BH_3)_3$ **1a** and **1b**, at least two M–B groupings are observed. The U–B distances between 2.683(8)–2.747(7) Å are consistent with κ^3-BH_3 coordination based on comparison to U–B distances and corresponding BH_3 denticities reported with U^{3+}.[52,87,88] The second grouping spans a slightly larger range from 2.892(6)–3.04(4) Å. These values are consistent primarily with κ^2 denticity,[52,87] although the largest M–B bond distance at 3.04 (4) Å may be κ^1 because it is slightly beyond what is typically reported for κ^2-BH_3 with U^{3+}. The structures of **2–4** show similar distributions of M–B distances, but the scatter of the longest bond distances become smaller as the metal radii decrease. Overall, the summation of the M–B distances suggest that the coordination numbers are 13–14, which is consistent with those reported previously for trivalent lanthanide and actinide ^{t}Bu-PDB complexes,[47,48] as well as other borohydride complexes.[43,52,87,89–91]

One of the more significant differences between the Ph-PDB structures is the B–P–B angles, which show remarkable flexibility and vary by as much as 15.4°. The polymeric structures for **1a** and **2** have larger chelating and bridging B–P–B angles compared to the dimeric structures for **1b**, **3**, and **4** (Fig. 5). The chelating B–P–B angles in the dimeric structures average 105.7(4)°, whereas those in the polymeric structures

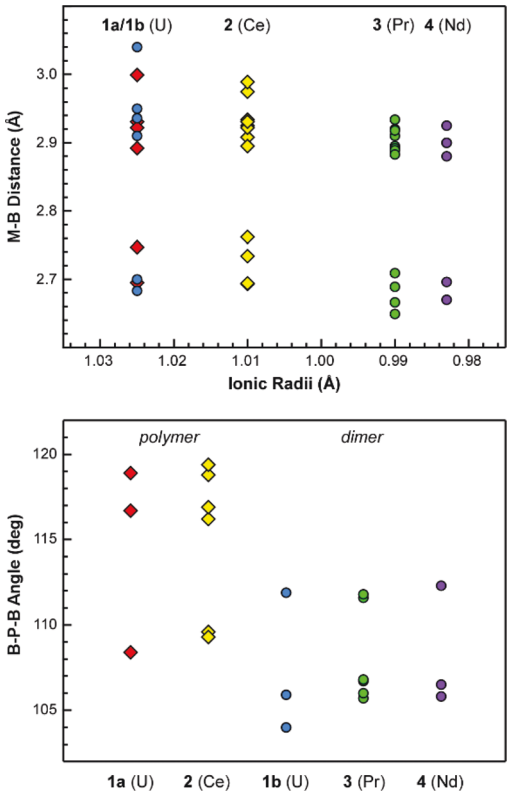

Fig. 5 Metal–boron (M–B) distances (top) and B–P–B angles (bottom) from single-crystal XRD data. Data points for polymeric structures are represented as diamonds whereas those for dimeric structures are represented as spheres.

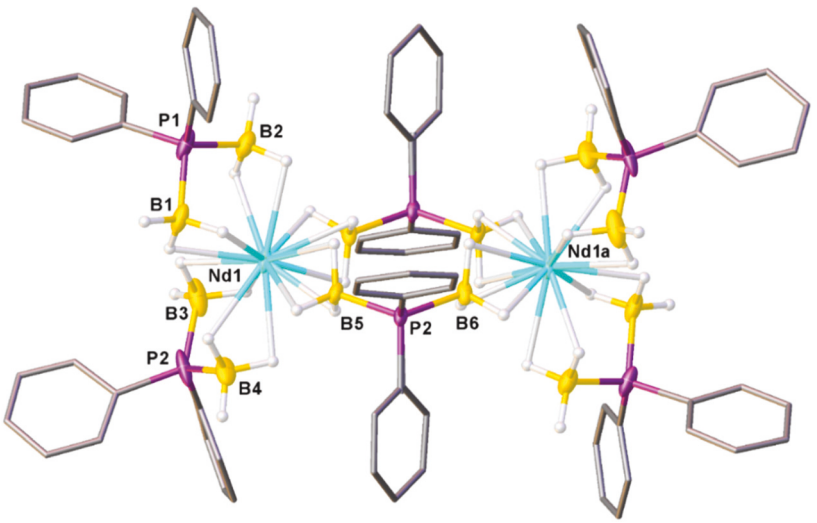

Fig. 4 Molecular structure of $Nd(H_3BPPh_2BH_3)_3$ (**4**). Ellipsoids shown at 35% probability. The phenyl rings are represented as pipes and hydrogens attached to carbon are omitted for clarity.

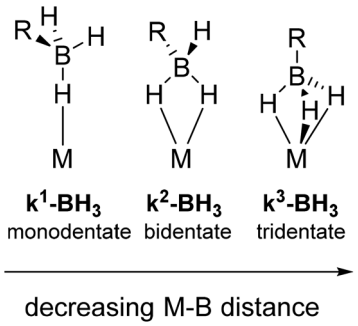

Chart 3 Comparison of B–H denticity and M–B distance.

average 109.1(2)°. Likewise, the bridging B–P–B angles in the dimers average 111.9(4)°, which is significantly smaller than the average bridging B–P–B angles in the polymeric structures at 117.8(2)°. In general, Ph-PDB can access a wider range of B–P–B angles than previously observed with ^{t}Bu-PDB complexes, which only vary by as much as 7.8°. Furthermore, all homoleptic ^{t}Bu-PDB complexes structurally characterized to date with trivalent f-metals – even those with U^{3+} and Ce^{3+} – exist as dimers in the solid state. We attribute these structural differences with Ph-PDB and ^{t}Bu-PDB to the decreased steric profile afforded by phenyl substituents, which can rotate and adopt different conformations to afford a wider range of B–P–B angles than with *tert*-butyl.

Synthesis and structure of $Nd(H_3BPPh_2BH_3)_3(THF)_3$

We have shown in previous studies that the ^{t}Bu-PDB complexes $U(H_3BP^tBu_2BH_3)_3$ and $Nd(H_3BP^tBu_2BH_3)_3$ could be crystallized as base-free dimers from THF-containing solutions.[47] In contrast, ^{t}Bu-PDB complexes with smaller lanthanides such as Tb $(H_3BP^tBu_2BH_3)_3$, $Er(H_3BP^tBu_2BH_3)_3$, and $Lu(H_3BP^tBu_2BH_3)_3$ all formed monomeric complexes with the formula $M(H_3BP^tBu_2BH_3)_3(THF)_3$, where M = Tb, Er, and Lu.[47] Dissolving crystals of $Nd(H_3BPPh_2BH_3)_3$ (**4**) in THF clearly yielded different ^{11}B resonances compared to those for **4**, which suggested that a new complex was formed. Indeed, this was confirmed by addition of Et_2O to the THF solutions, which yielded light purple XRD quality crystals of $Nd(H_3BPPh_2BH_3)_3(THF)_3$ (**4-THF**; Fig. 6).

The coordination geometry of **4-THF** is pentagonal bipyramidal based on the arrangement of the boron and oxygen atoms around Nd. This differs from the THF adducts previously observed with ^{t}Bu-PDB complexes containing smaller lanthanides because it contains two dangling and one chelating Ph-PDB ligands instead of three dangling ligands (Fig. 6). These structural differences are likely attributed to the increased radii and larger coordination sphere of Nd^{3+} compared to Tb^{3+}, Er^{3+}, and Lu^{3+}. The chelating Ph-PDB ligand in **4-THF** lies in the equatorial plane with the three THF molecules. Both BH_3 groups coordinate in a bidentate fashion with representative Nd–B distances of 2.990(9) and 2.908(8) Å. The two dangling Ph-PDB ligands occupy the axial positions with each BH_3 group bound

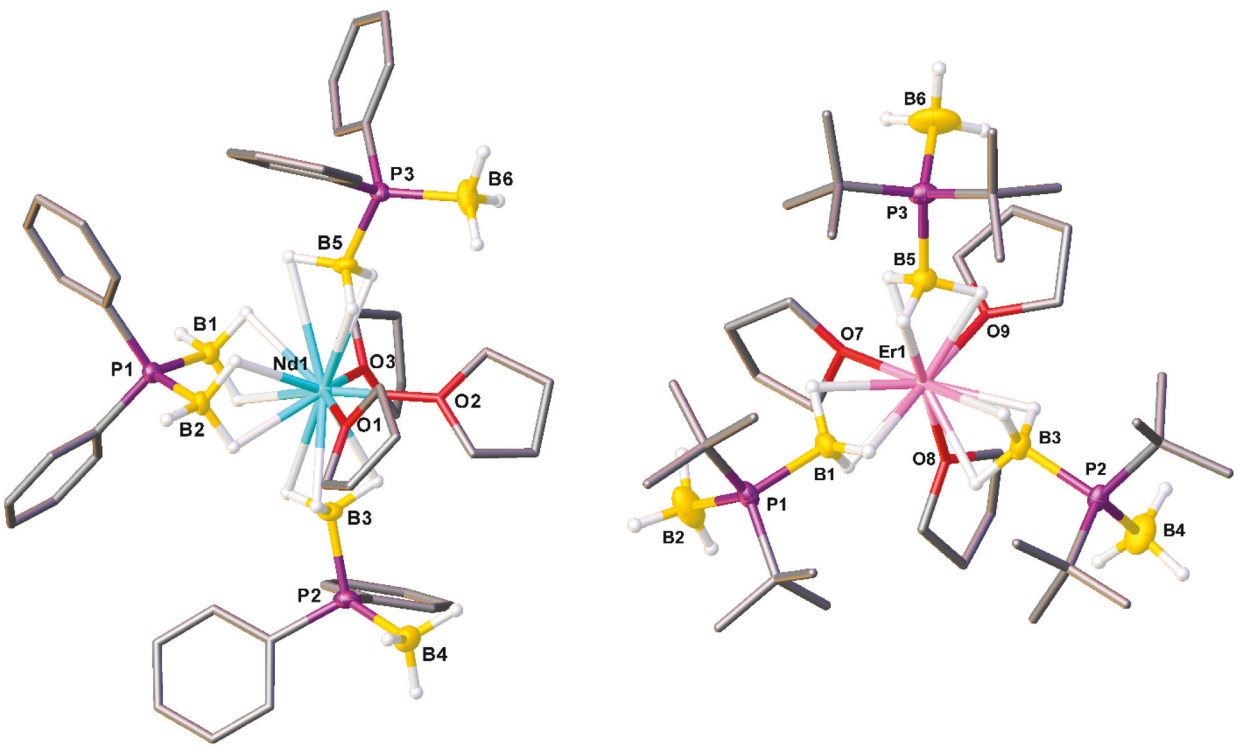

Fig. 6 Single-crystal XRD structure comparison between $Nd(H_3BPPh_2BH_3)_3(THF)_3$ (**4-THF**; left) and $Er(H_3BP^tBu_2BH_3)_3(THF)_3$ (right).[47] Thermal ellipsoids are drawn with 35% probability. All phenyl rings, *tert*-butyl groups, and THF molecules are represented as pipes and all hydrogen atoms attached to carbon were omitted from the figure.

in a tridentate fashion, as indicated by the shorter Nd–B distances of 2.678(8) and 2.791(7) Å (Table 1). The average Nd–O bond distance of 2.49(6) Å is consistent with other Nd^{3+} complexes containing THF ligands. The overall coordination number of **4-THF** is 13 when considering the denticity of the BH_3 groups.

Despite the different substituents attached to phosphorus, the B–P–B angles and associated intramolecular B···B distances in the dangling Ph-PDB ligands in **4-THF** and ^{t}Bu-PDB complexes such as $Er(H_3BP^tBu_2BH_3)_3(THF)_3$ are effectively identical in the absence of chelation or intermolecular bridging modes.

Spectroscopic analysis of Ph-PDB complexes

^{1}H and ^{11}B NMR data were collected on all the Ph-PDB complexes to analyze their structures in solution. As reported for ^{t}Bu-PDB complexes, and despite the differences in solid-state structures, homoleptic Ph-PDB complexes appear to exist as a mixture of monomers and dimers in solution (Scheme 2).[47,48] The ^{1}H and ^{11}B NMR spectra revealed three paramagnetically shifted BH_3 resonances for each compound (Table 2). Two of these resonances exist in a 1 : 2 ratio consistent with the different chemical environments expected for the bridging and chelating Ph-PDB ligands in the dimer, whereas the remaining resonance is assigned to chemically equivalent Ph-PDB ligands in the monomer. The ^{1}H NMR spectra also showed a range of different phenyl resonances, although these were less paramagnetically shifted than the BH_3 resonances and more difficult to assign due to the monomer/dimer mixture, different hydrogen positions on each phenyl group, and overlap of different resonances.

^{11}B NMR data for the THF bound and unbound species, **4-THF** and **4**, show very different NMR spectra in CD_2Cl_2 (Fig. 7). As noted above, $Nd(H_3BPPh_2BH_3)_3$ shows three well defined resonances with the BH_3 resonances of the chelating and bridging Ph-PDB ligands of the dimer at δ 176.5 and 75.6, respectively. The middle resonance at δ 95.3 is assigned to the monomer. The ^{11}B NMR spectrum of **4-THF** also shows three features, but at significantly higher field at δ 71.8, 55.0, and 45.4 ppm. These three resonances are consistent with the presence of three unique BH_3 environments in the monomeric structure of **4-THF**.

Table 2 Room temperature ^{1}H and ^{11}B NMR data of BH_3 resonances (δ, ppm) for Ph-PDB complexes in CD_2Cl_2

	Dimer		Monomer	
Complex	^{1}H	^{11}B	^{1}H	^{11}B
1	70.2, 94.1	130.7, 308.4	93.0	186.3
2	20.8, 33.1	3.1, 44.0	23.8	11.4
3	55.8, 79.0	46.3, 147.2	63.8	66.1
4	77.3, 83.5	75.6, 176.5	78.3	95.3

Solid-state IR data were collected on Ph-PDB complexes to assess the effect that structural variations and THF binding have on molecular vibrations, especially B–H stretching frequencies that appear between 2200 cm^{-1} and 2500 cm^{-1} (Fig. 8). Spectra collected on the homoleptic base-free complexes show only subtle variations across the series despite the structural differences between the polymers (**1a** and **2**) and the dimers (**1b**, **3**, and **4**). Each spectrum yielded a strong B–H stretching band centered around 2250 cm^{-1} that is assigned to bridging B–H–M stretches. Two more resolved, albeit less intense vibrations, were observed at higher wavenumbers and assigned to terminal B–H stretches (*ca.* 2440 cm^{-1}). In contrast to the base-free complexes, the IR spectrum of **4-THF** revealed new B–H stretches at 2331 and 2358 cm^{-1} consistent with the dangling BH_3 groups. The spectrum of **4-THF** also revealed the diagnostic symmetric and asymmetric C–O–C vibrations associated with THF at 853 and 1003 cm^{-1}, respectively, and additional C–H stretches close to 3000 cm^{-1}.

As previously observed for the $M(H_3BP^tBu_2BH_3)_3(THF)_3$ complexes with ^{t}Bu-PDB, the THF molecules in **4-THF** can be displaced to some extent by placing the samples under vacuum or by vigorously grinding the sample with KBr. This

Table 1 Bond distance and angle measurements for $Nd(H_3BPPh_2BH_3)_3(THF)_3$ (**4-THF**)

Ln–B	Ln–O	B···B	B–P–B	B–Nd–B		B–Ln–O		
2.990(9)	2.47(1)	3.112(9)	107.5(3)	63.7(2)	94.7(2)	151.9(2)	74.8(2)	87.1(3)
2.908(8)	2.479(5)	3.24(1)	114.6(4)	98.8(2)	96.7(2)	137.4(3)	73.9(3)	91.0(3)
2.678(8)	2.506(3)	3.22(1)	115.1(4)	91.0(2)	167.4(2)	144.0(2)	84.6(2)	82.3(2)
2.791(7)						137.9(2)	85.3(2)	90.4(2)

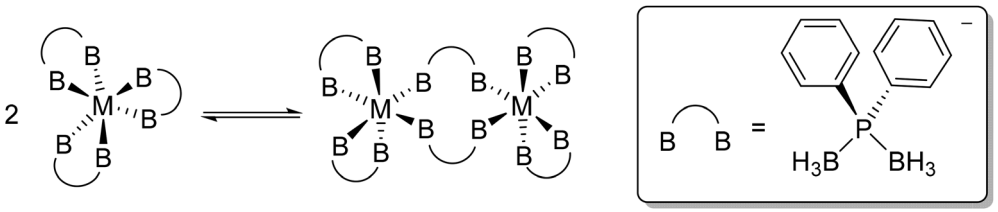

Scheme 2 Comparison of monomeric and dimeric phosphinodiboranate complexes presumed to exist in solution.

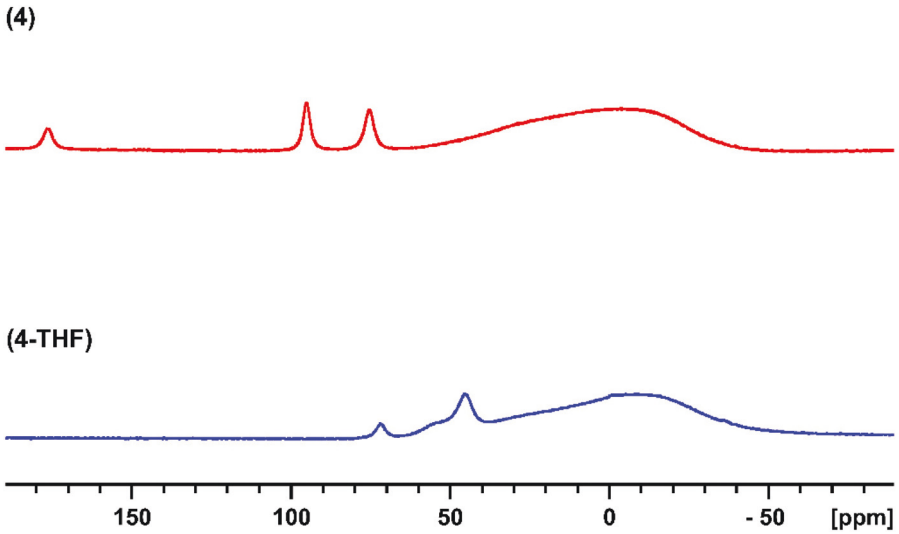

Fig. 7 ^{11}B NMR stack plot of $Nd(H_3BPPh_2BH_3)_3$ (**4**) and $Nd(H_3BPPh_2BH_3)_3(THF)_3$ (**4-THF**). Data for both complexes were collected in CD_2Cl_2. The broad feature centered around δ 0 ppm is attributed to borosilicate inside the instrument.

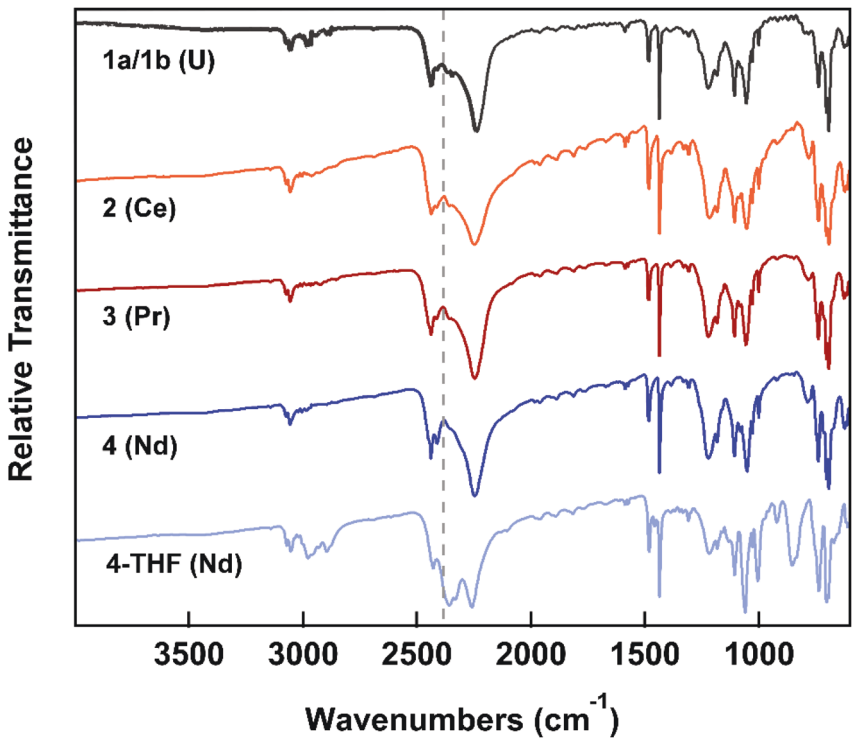

Fig. 8 Comparison of solid-state IR data (KBr) for **1a/1b**, **2**, **3**, **4**, and **4-THF**. The gray dashed line was added at 2400 cm^{-1} for reference.

was observed during our initial attempts to prepare IR samples of **4-THF** as KBr pellets. These samples yielded spectra identical to the base–free complex **4** and showed no THF vibrations. For this reason, the solid-state IR spectrum of **4-THF** was only lightly ground prior to pellet formation. Attenuated total reflectance (ATR) IR data were also collected for all the complexes and were in good agreement with the KBr data (see supporting information).

Synthesis and XRD studies of $U(H_3BPH_2BH_3)I_2(THF)_3$

In sharp contrast to our results with $K(H_3BPPh_2BH_3)$, attempts to prepare homoleptic H-PDB complexes using $Na(H_3BPH_2BH_3)$ were less productive. For example, grinding $UI_3(THF)_4$ with more than three equivalents of $Na(H_3BPH_2BH_3)$ yielded only the partial metathesis product $U(H_3BPH_2BH_3)I_2(THF)_3$ (**5**). The complex was isolated by extraction with chlorobenzene and sub-

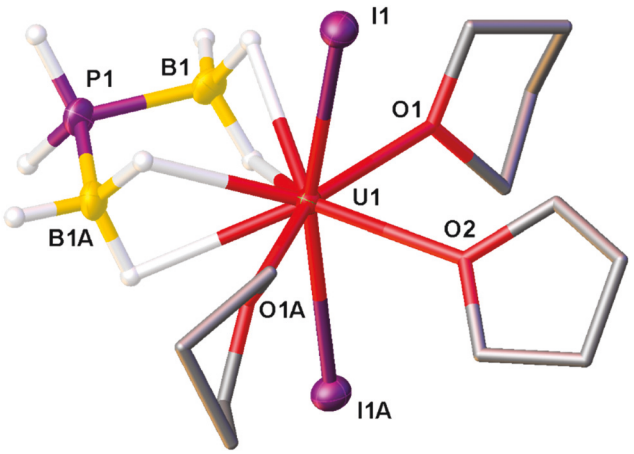

Fig. 9 Single crystal XRD structure of $U(H_3BPH_2BH_3)I_2(THF)_3$ (**5**). Thermal ellipsoids are shown at 35% probability. THF ligands are represented as pipes and hydrogen atoms attached to THF were omitted from the figure.

sequently crystallized from THF and pentane in very low yields (≤6%). Attempts to use other extracting solvents (Et_2O, DCM, and fluorobenzene) yielded no soluble product. Synthesis of the neodymium congener was also attempted using the same method. As with **5**, the reaction was poor yielding and we were unable to obtain single crystals for XRD analysis.

Single-crystal XRD studies of **5** revealed a distorted pentagonal bipyramidal coordination geometry with the two iodide ligands in the axial positions and the H-PDB and THF ligands occupying the equatorial plane (Fig. 9). The U–B distances of 2.965 Å indicate κ^2 coordination of the BH_3 groups, as observed in **1a** and **1b**. The *trans* I–U–I bond angle is bent slightly away from the H-PDB ligand at 164.3(4)°. The H-PDB anion has a B–P–B angle of 106.7(8)°, which is close to the angle observed for the chelating B–P–B angles in both $U(H_3BPPh_2BH_3)_3$ structures (**1a** and **1b**). The structure of **5** is remarkably similar to Er $(H_3BNH_2BH_3)Cl_2(THF)_3$ containing the unsubstituted aminodiboranate (and N congener) $H_3BNH_2BH_3^-$.[53] It is worth noting that $Er(H_3BNH_2BH_3)Cl_2(THF)_3$ was also isolated as an incomplete metathesis product in attempts to prepare Er $(H_3BNH_2BH_3)_3$, and similar results have been observed with Nd $(H_3BNMe_2BH_3)Cl_2(THF)_3$ (as discussed in more detail below).[54]

Conclusion

In summary, we have demonstrated how mechanochemistry can be used to overcome limited solution reactivity for the synthesis of f-metal phosphinodiboranate complexes $U(H_3BPPh_2BH_3)_3$ (**1**), $Ce(H_3BPPh_2BH_3)_3$ (**2**), $Pr(H_3BPPh_2BH_3)_3$ (**3**), and $Nd(H_3BPPh_2BH_3)_3$ (**4**). Single-crystal XRD studies showed that these complexes exist as coordination polymers (**1a** and **2**) or dimers (**1b**, **3**, and **4**) in the solid state, but they depolymerize and appear to exist as mixtures of monomers and dimers in solution according to ^1H and ^{11}B NMR studies. Despite the success with Ph-PDB, only the partial metathesis product $U(H_3BPPH_2BH_3)I_2(THF)_2$ (**5**) was isolated when similar mechanochemical reactions were attempted using the unsubstituted phosphinodiboranate salt Na(H-PDB).

The biggest question that remains from these studies is: why do metathesis reactions with some PDB salts work when performed under mechanochemical conditions but fail when performed in solution, especially with THF or Et_2O? We can speculate on this question by comparing our results to studies with aminodiboranates (the N congeners of phosphinodiboranates) that showed how salt elimination reactions with trivalent f-metal halides can be attenuated (and even reversed!) when performed in coordinating solvents. It was recently reported that mixing $NdCl_3$ with three equiv. of Na $(H_3BNMe_2BH_3)$ in THF yields a mixture containing the partial metathesis product $Nd(H_3BNMe_2BH_3)Cl_2(THF)_3$.[54] Subsequent removal of the solvent from the mixture – which still contained unreacted $Na(H_3BNMe_2BH_3)$ – followed by addition of non-coordinating pentane to the solid residue allowed the metathesis reactions to proceed to completion with rapid formation of $Nd(H_3BNMe_2BH_3)_3(THF)$.[54] More remarkably, it was shown that dissolving $Nd(H_3BNMe_2BH_3)_3(THF)$ in THF with a suspension of excess NaCl (which has very poor solubility in THF at 6 mg L^{-1})[54] yielded $Nd(H_3BNMe_2BH_3)Cl_2(THF)_3$ with elimination of 2 equiv. of $Na(H_3BNMe_2BH_3)$. These results clearly indicate that $Nd(H_3BNMe_2BH_3)Cl_2(THF)_3$ is the thermodynamically-favored product in THF when both NaCl and Na $(H_3BNMe_2BH_3)$ are present. Interestingly, performing the same reaction by mixing $NdCl_3$ with three equiv. of Na $(H_3BNMe_2BH_3)$ in more weakly-coordinating Et_2O instead of THF allowed the metathesis reaction to proceed to completion to form $Nd(H_3BNMe_2BH_3)_3$. Similar solvent-dependent differences in salt elimination reactivity were observed for the synthesis of $U(H_3BNMe_2BH_3)_3(THF)$ and $U(H_3BNMe_2BH_3)_3$ in THF and Et_2O, respectively.[52]

While different thermodynamic (*e.g.*, solvation, lattice energy, metal–ligand bond strength) and kinetic factors contribute to determining whether a metathesis reaction occurs,[54] a key factor governing these reactions appears to be the strength of metal-solvent coordination relative to the incoming ligand. Donor solvents, which also exist in large excess in solution-phase reactions, must be displaced from the metal along with the corresponding halide for a metathesis reaction to proceed. Compared to reactions with $Na(H_3BNMe_2BH_3)$, this appears to be even more problematic for the Ph-PDB salt, which did not exhibit any observable reactivity in THF or Et_2O with the trivalent f-metal iodides tested here. The metathesis reactions do proceed slowly in chlorobenzene, but also fail to go to completion at RT within 24 h, which suggests that even chlorobenzene may impede reaction progress in solution. In the context of this hypothesis, it has been shown that neutral, substituted benzenes like chlorobenzene can coordinate to trivalent f-metals,[92,93] and examples of arene-bound U^{3+} complexes containing borohydride ligands have been structurally characterized.[94,95] More work is needed to fully elaborate all the factors contributing to limited PDB salt metathesis reactivity in solution, but the comparative Ph-PDB studies described

here provide another example showing how mechanochemistry can facilitate access to metal complexes that are otherwise difficult to prepare by conventional solution methods.

Experimental

General considerations

All reactions were carried out under an atmosphere of N_2 using glovebox or standard Schlenk techniques. All glassware was heated at 150 °C for at least two hours and allowed to cool under vacuum before use. Solvents were dried and deoxygenated using a Pure Process Technologies Solvent Purification System and stored over 3 Å molecular sieves. Deuterated solvents were deoxygenated on the Schlenk line by three freeze–pump–thaw cycles and stored over 3 Å molecular sieves for at least 3 days before use. $K(H_3BPPh_2BH_3)$ and $Na(H_3BPH_2BH_3)$ were prepared from commercially available starting materials using reported methods.[73,74,77] $UI_3(THF)_4$ was prepared from $UI_3(1,4\text{-dioxane})_{1.5}$, as described by Kiplinger and coworkers,[96] or from UCl_4 as described by us.[97] Anhydrous LnI_3 salts were purchased from Alfa Aesar or Strem Chemicals and used as received.

^{1}H NMR data were collected on a Bruker AVANCE-400 operating at 400 MHz, or a Bruker AVANCE-500 operating at 500 MHz. The ^{11}B NMR data were collected on a Bruker AVANCE-400 operating at 128 MHz or a Bruker AVANCE-500 operating at 160 MHz. Chemical shifts are reported in δ units relative to residual NMR solvent peaks (^{1}H) or $BF_3{\cdot}Et_2O$ (^{11}B; δ 0.0 ppm). ^{31}P NMR resonances were not observed for any of the metal complexes presumably because of unresolved peak broadening in the presence of paramagnetic metals and quadrupolar coupling with the boron nuclei (^{11}B and ^{10}B). Microanalytical data (CHN) were collected using an EAI CE-440 elemental analyzer at the University of Iowa's Shared Instrumentation Facility. CHN analysis for all the complexes gave satisfactory %H, but %C data were consistently 2–4% lower than expected for all the complexes, which may be attributed to metal-carbide formation during combustion. IR spectra were acquired with a Thermo Scientific Nicolet iS5 in an N_2-filled glovebox as KBr pellets or using an ATR accessory. Mechanochemical reactions were carried out on a Form-Tech Scientific (FTS) FTS1000 shaker mill operating at 1800 rpm. All mechanochemical reactions were conducted in 5 mL stainless steel FTS "SmartSnap" grinding jars using two 5 mm stainless steel balls (304 grade) for grinding. The average weight of the balls was 0.522 ± 0.002 g based on measurement and averaging of 5 samples.

Tris(diphenylphosphinodiboranato)uranium(III), $U(H_3BPPh_2BH_3)_3$ (1). $UI_3(THF)_4$ (0.101 g, 0.111 mmol) and $K(H_3BPPh_2BH_3)$ (0.0834 g, 0.331 mmol) were loaded into a 5 mL FTS ball milling jar with two 5 mm stainless steel balls and several drops of Et_2O. The jar was hermetically sealed, transferred to an FTS shaker mill, and milled for 90 minutes. The jar was then transferred to a glovebox and opened to reveal a dark red residue. The contents were scraped into an 11-dram vial equipped with a stir bar and stirred in 40 mL of fluorobenzene for 30 minutes. The suspension was filtered through a fine frit and evaporated to dryness under vacuum to reveal a red oily solid. The solid was dissolved in the minimal amount of DCM (*ca.* 1 mL) and slowly diffused with Et_2O to afford small dark red needles (38 mg). Yield: 46%. Anal. Calcd for $C_{36}H_{48}B_6P_3U$: H, 5.52. Found: H, 5.46%. ^{1}H NMR (500 MHz, CD_2Cl_2): δ 6.09 (br s), 6.79 (br s), 7.30 (br s), 7.47 (br s), 7.59 (br s), 7.73 (br s), 8.08 (br s), 8.24 (br s), 70.2 (br s, FWHM = 640 Hz, 6H, BH_3, dimer), 93.0 (br s, FWHM = 550 Hz, 18H, BH_3, monomer), 94.1 (br s, FWHM = 470 Hz, 12H, BH_3, dimer). ^{11}B NMR (160 MHz, CD_2Cl_2): δ 130.7 (br s, FWHM = 500 Hz, BH_3, dimer), 186.3 (br s, FWHM = 660 Hz, BH_3, monomer), 308.4 (br s, FWHM = 380 Hz, BH_3, dimer). IR (KBr) $\bar{\nu}_{max}$ (cm^{-1}): 3075 (w), 3058 (w), 3006 (w), 2928 (w), 2853 (w), 2435 (m), 2412 (m), 2236 (s), 1981 (w), 1962 (w), 1885 (w), 1812 (w), 1761 (w), 1672 (w), 1586 (w), 1573 (w), 1482 (m), 1435 (s), 1384 (w), 1330 (w) 1307 (w), 1214 (s), 1183 (s), 1106(s), 1047 (s), 1027 (m), 999 (m), 921 (w), 845 (w), 780 (w), 746 (s), 746 (s), 701 (s), 690 (s), 622 (m), 612 (m).

Tris(diphenylphosphinodiboranato)cerium(III), $Ce(H_3BPPh_2BH_3)_3$ (2). Prepared as described for **1** with CeI_3 (0.103 g, 0.198 mmol) and $K(H_3BPPh_2BH_3)$ (0.145 g, 0.575 mmol). Yield: 53 mg (52%). Anal. Calcd for $C_{36}H_{48}B_6P_3Ce$: H, 6.21%. Found: H, 6.18%. ^{1}H NMR (500 MHz, CD_2Cl_2): δ 6.69 (br s), 7.18 (br s), 7.36 (br s), 7.76 (br s), 8.64 (br s), 20.8 (br s, FWHM = 480 Hz, 12H, BH_3, dimer), 23.8 (br s, FWHM = 420 Hz, 18H, BH_3, monomer), 33.1 (br s, FWHM = 470 Hz, 6H, BH_3, dimer). ^{11}B NMR (160 MHz, CD_2Cl_2): δ 3.1 (br s, FWHM = 440 Hz, BH_3, dimer), 11.4 (br s, FWHM = 370 Hz, BH_3, monomer), 44.0 (br s, FWHM = 510 Hz, BH_3, dimer). IR (KBr) $\bar{\nu}_{max}$ (cm^{-1}): 3144 (w), 3074 (w), 3057 (m), 3022 (w), 3005 (w), 2963 (w), 2438 (m), 2413 (m), 2357 (m), 2249 (s), 1961 (w), 1885 (w), 1812 (w), 1762 (w), 1671 (w), 1617 (w), 1586 (w), 1572 (w), 1539 (w), 1482 (m), 1435 (s), 1384 (w), 1330 (w), 1307 (w), 1216 (s), 1183 (s), 1106 (w), 1084 (m), 1052 (s), 1027 (m), 999 (m), 921 (w), 848 (w), 781 (w), 738 (s), 703 (s), 691 (s), 623 (m), 612 (m).

Tris(diphenylphosphinodiboranato)praseodymium(III), $Pr(H_3BPPh_2BH_3)_3$ (3). Prepared as described for **1** with PrI_3 (0.105 g, 0.201 mmol) and $K(H_3BPPh_2BH_3)$ (0.145 g, 0.575 mmol). Yield: 105 mg (83%). Anal. Calcd for $C_{36}H_{48}B_6P_3Pr$: H, 6.21%. Found: H, 5.96%. ^{1}H NMR (500 MHz, CD_2Cl_2): δ 5.85 (br s), 6.76 (br s), 6.88 (br s), 7.33 (br s), 7.61 (br s), 10.09 (br s), 55.8 (br s, FWHM = 500 Hz, 12H, BH_3, dimer), 63.8 (br s, FWHM = 550 Hz, 18H, BH_3, monomer), 79.0 (br s, FWHM = 300 Hz, 6H, BH_3, dimer). ^{11}B NMR (160 MHz, CD_2Cl_2): δ 46.3 (br s, FWHM = 370 Hz, BH_3, dimer), 66.1 (br s, FWHM = 380 Hz, BH_3, monomer), 147.2 (br s, FWHM = 340 Hz, BH_3, dimer). IR (KBr) $\bar{\nu}_{max}$ (cm^{-1}): 3074 (w), 3058 (w), 2921 (w), 2853 (w), 2436 (m), 2412 (m), 2244 (s), 2138 (w), 1982 (w), 1962 (w), 1886 (w), 1812 (w), 1761 (w), 1672 (w), 1586 (w), 1572 (w), 1482 (m), 1434 (s), 1384 (w), 1330 (w), 1307 (w), 1213 (s), 1183 (s), 1106 (s), 1080 (w), 1049 (s), 1027 (m), 999 (s), 921 (w), 865 (w), 844 (w), 782 (m), 746 (s), 701 (s), 690 (s), 622 (s), 612 (s).

Tris(diphenylphosphinodiboranato)neodymium(III), $Nd(H_3BPPh_2BH_3)_3$ (4). Prepared as described for **1** with NdI_3 (0.102 g, 0.194 mmol) and $K(H_3BPPh_2BH_3)$ (0.143 g, 0.568 mmol). Yield: 96.6 mg (77%). Anal. Calcd for $C_{36}H_{48}B_6P_3Nd$: H, 6.18%. Found: H, 6.00%. ^{1}H NMR (400 MHz, CD_2Cl_2): δ 7.47 (br s), 7.73 (br s), 8.17 (br s), 77.3 (br s, FWHM = 550 Hz, 6H, BH_3, dimer), 78.3 (br s, FWHM = 520 Hz, 18H, BH_3, monomer), 83.5 (br s, FWHM = 510 Hz, 12H, BH_3, dimer). ^{11}B NMR (128 MHz, CD_2Cl_2): δ 75.6 (br s, FWHM = 490 Hz, BH_3, dimer), 95.3 (br s, FWHM = 390 Hz, BH_3, monomer), 176.5 (br s, FWHM = 440 Hz, BH_3 dimer). IR (KBr) $\bar{\nu}_{max}$ (cm^{-1}): 3074 (w), 3057 (w), 3021 (w), 3005 (w), 2986 (w), 2438 (m), 2412 (m), 2247 (m) 1983 (w), 1961 (w), 1885 (w), 1812 (w), 1761 (w), 1671 (w), 1482 (w), 1435 (s), 1384 (w), 1330 (w), 1307 (w), 1221 (s), 1183 (s), 1107 (s), 1080 (m), 1050 (s), 999 (m), 9279 (w), 845 (w), 785 (m), 740 (m), 702 (s), 692 (s), 623 (m), 626 (m).

Tris(diphenylphosphinodiboranato)tris(tetrahydrofuran)neodymium(III), $Nd(H_3BPPh_2BH_3)_3(THF)_3$ (4-THF). In a 2-dram vial, 0.050 g of **4** was dissolved in THF (*ca.* 1 mL). Vapor diffusion with Et_2O yielded small light purple blocks the next morning. Yield: 58 mg (67%). ^{1}H NMR (400 MHz, CD_2Cl_2): δ 4.54 (br s), 5.51 (br s), 6.87 (s), 7.03 (s), 7.43 (br s), 47.7 (br s, FWHM = 1100 Hz, BH_3), 50.7 (br s, FWHM = 1200 Hz, BH_3), 64.8 (br s, FWHM = 670 Hz, BH_3). ^{11}B NMR (128 MHz, CD_2Cl_2): δ 45.4 (br s, FWHM = 820 Hz, BH_3), 55.0 (br s, FWHM = 660 Hz, BH_3), 71.8 (br s, FWHM = 470 Hz, BH_3). IR (KBr) $\bar{\nu}_{max}$ (cm^{-1}): 3073 (w), 3054 (m), 2978 (m), 2896 (m), 2428 (m), 2358 (s), 2331 (s), 2259 (s), 1962 (s), 1890 (s), 1816 (s), 1772 (s), 1673 (s), 1586 (s), 1572 (s), 1481 (m), 1457 (w), 1435 (s), 1386 (w), 1367 (w), 1346 (w), 1332 (w), 1308 (w), 1217 (m), 1182 (m), 1159 (w), 1132 (w), 1106 (m), 1059 (s), 1028 (m), 1003 (s, THF), 978 (w), 921 (m), 853 (m, THF), 736 (s), 702 (s), 694 (s), 669 (m), 618 (m).

Diiodo(phosphinodiboranato)tris(tetrahydrofuran)uranium(III), $U(H_3BPH_2BH_3)I_2(THF)_3$ (5). $UI_3(THF)_4$ (0.100 g, 0.111 mmol) and $Na(H_3BPH_2BH_3)$ (0.0331 g, 0.396 mmol) were loaded into a 5 mL FTS ball milling jar with two 5 mm stainless steel balls and several drops of Et_2O. The jar was hermetically sealed, placed on the FTS shaker mill, and milled for three hours. The jar was transferred into a glovebox and opened to reveal a dark red brown paste. The contents were extracted with 20 mL of chlorobenzene, stirred to homogenize, then filtered over a fine frit. The residue was washed with copious amounts of chlorobenzene (*ca.* 60 mL) then stripped down to dryness to reveal a red oil. The oil was dissolved in the minimal amount of THF (*ca.* 1 mL), and vapor diffused with pentane to yield small red blocks the following day. Yield: 5.3 mg (6.2%). IR (ATR) $\bar{\nu}_{max}$ (cm^{-1}): 2989 (w), 2920 (m), 2853 (m), 2438 (m), 2401 (w), 2368 (m), 2240 (m), 1456 (w), 1436 (w), 1377 (w), 1365 (w), 1342 (w), 1294 (w), 1218 (m), 1177 (w), 1147 (w), 1058 (s), 1004 (s, THF), 917 (w), 887 (m), 835 (s, THF), 666 (m).

XRD studies

Suitable crystals for single-crystal X-ray diffraction were grown from either DCM and Et_2O (**1a** and **1b**, **2**, **3**, and **4**), THF and Et_2O (**4-THF**), or THF and pentane (**5**) and mounted on a MiTeGen micromount with ParatoneN oil. Crystallographic data were collected using a Bruker Nonius Kappa ApexII, equipped with a charge-coupled-device (CCD) detector and cooled to 150 K using an Oxford Cryostreams 700 low temperature device or a Bruker D8 Venture Duo, equipped with a Bruker photon III detector and cooled to 150 K using an Oxford Cryostreams 800C low temperature device. Data were collected with MoK_α radiation (λ = 0.71073 Å). A hemisphere of data was collected using phi and omega scans. The data were corrected for absorption using redundant reflections and the SADABS program.[98] Structures were solved with intrinsic phasing (SHELXT) and least square refinement (SHELXL) confirmed the positions of all non-hydrogen atoms.[98] All hydrogen atom positions were idealized and were allowed to ride on the attached carbon and boron atoms. B–H bond distances were fixed at 1.2 Å. Structure solution and refinement were performed with Olex2.[99]

Conflicts of interest

There are no conflict to declare.

Acknowledgements

This material is based upon work supported by the US Department of Energy (DOE), Office of Science, Office of Basic Energy Sciences, Separation Science program under award DESC0019426. The NSF is gratefully acknowledged for supporting the purchase of a new X-ray diffractometer under award CHE-1828117. We thank Dale Swenson for collecting the single-crystal XRD data. T. V. F. would also like to thank Amy Charles for her assistance in the organization and revisions of this manuscript *via* the UIowa Chemistry reading and writing group. T. V. F. also gratefully acknowledges a post comprehensive exam fellowship from the University of Iowa Graduate College.

References

1 J. F. Fernandez-Bertran, *Pure Appl. Chem.*, 1999, **71**, 581–586.
2 M. K. Beyer and H. Clausen-Schaumann, *Chem. Rev.*, 2005, **105**, 2921–2948.
3 G. Kaupp, *CrystEngComm*, 2009, **11**, 388–403.
4 S. L. James, C. J. Adams, C. Bolm, D. Braga, P. Collier, T. Friscic, F. Grepioni, K. D. M. Harris, G. Hyett, W. Jones, A. Krebs, J. Mack, L. Maini, A. G. Orpen, I. P. Parkin, W. C. Shearouse, J. W. Steed and D. C. Waddell, *Chem. Soc. Rev.*, 2012, **41**, 413–447.
5 E. Boldyreva, *Chem. Soc. Rev.*, 2013, **42**, 7719–7738.
6 L. Takacs, *Chem. Soc. Rev.*, 2013, **42**, 7649–7659.
7 W. Jones and M. D. Eddleston, *Faraday Discuss.*, 2014, **170**, 9–34.
8 J.-L. Do and T. Friscic, *ACS Cent. Sci.*, 2017, **3**, 13–19.

9 T. Friscic, C. Mottillo and H. M. Titi, *Angew. Chem.*, 2020, **59**, 1018–1029.
10 B. G. Fiss, A. J. Richard, G. Douglas, M. Kojic, T. Friscic and A. Moores, *Chem. Soc. Rev.*, 2021, **50**, 8279–8318.
11 K. Horie, M. Barón, R. B. Fox, J. He, M. Hess, J. Kahovec, T. Kitayama, P. Kubisa, E. Maréchal, W. Mormann, R. F. T. Stepto, D. Tabak, J. Vohlídal, E. S. Wilks and W. J. Work, *Pure Appl. Chem.*, 2004, **76**, 889–906.
12 *IUPAC, Compendium of Chemical Terminology*, Compiled by A. D. McNaught and A. Wilkinson. Blackwell Scientific Publications, Oxford 2nd ed, (the "Gold Book") 1997.
13 A. L. Garay, A. Pichon and S. L. James, *Chem. Soc. Rev.*, 2007, **36**, 846–855.
14 G.-W. Wang, *Chem. Soc. Rev.*, 2013, **42**, 7668–7700.
15 J. G. Hernandez and T. Friscic, *Tetrahedron Lett.*, 2015, **56**, 4253–4265.
16 N. R. Rightmire and T. P. Hanusa, *Dalton Trans.*, 2016, **45**, 2352–2362.
17 J. G. Hernandez and C. Bolm, *J. Org. Chem.*, 2017, **82**, 4007–4019.
18 A. A. Geciauskaite and F. Garcia, *Beilstein J. Org. Chem.*, 2017, **13**, 2068–2077.
19 V. Strukil, *Synlett*, 2018, **29**, 1281–1288.
20 J. L. Howard, Q. Cao and D. L. Browne, *Chem. Sci.*, 2018, **9**, 3080–3094.
21 D. Tan and T. Friscic, *Eur. J. Org. Chem.*, 2018, 18–33.
22 A. Beillard, X. Bantreil, T.-X. Métro, J. Martinez and F. Lamaty, *Chem. Rev.*, 2019, **119**, 7529–7609.
23 A. Bose and P. Mal, *Beilstein J. Org. Chem.*, 2019, **15**, 881–900.
24 D. Tan and F. Garcia, *Chem. Soc. Rev.*, 2019, **48**, 2274–2292.
25 D. Braga, S. L. Giaffreda, F. Grepioni, A. Pettersen, L. Maini, M. Curzi and M. Polito, *Dalton Trans.*, 2006, 1249–1263.
26 P. Balaz, M. Achimovicova, M. Balaz, P. Billik, Z. Cherkezova-Zheleva, J. M. Criado, F. Delogu, E. Dutkova, E. Gaffet, F. J. Gotor, R. Kumar, I. Mitov, T. Rojac, M. Senna, A. Streletskii and K. Wieczorek-Ciurowa, *Chem. Soc. Rev.*, 2013, **42**, 7571–7637.
27 C. Xu, S. De, A. M. Balu, M. Ojeda and R. Luque, *Chem. Commun.*, 2015, **51**, 6698–6713.
28 E. L. Dreizin and M. Schoenitz, *J. Mater. Sci.*, 2017, **52**, 11789–11809.
29 P. Zhang and S. Dai, *J. Mater. Chem. A*, 2017, **5**, 16118–16127.
30 Y.-R. Miao and K. S. Suslick, *Adv. Inorg. Chem.*, 2018, **71**, 403–434.
31 M. J. Munoz-Batista, D. Rodriguez-Padron, A. R. Puente-Santiago and R. Luque, *ACS Sustainable Chem. Eng.*, 2018, **6**, 9530–9544.
32 D. Chen, J. Zhao, P. Zhang and S. Dai, *Polyhedron*, 2019, **162**, 59–64.
33 A. Delori, T. Friscic and W. Jones, *CrystEngComm*, 2012, **14**, 2350–2362.
34 M. Perez-Venegas and E. Juaristi, *ACS Sustainable Chem. Eng.*, 2020, **8**, 8881–8893.
35 J.-L. Do and T. Friscic, *Synlett*, 2017, **28**, 2066–2092.
36 K. J. Ardila-Fierro and J. G. Hernandez, *ChemSusChem*, 2021, **14**, 2145–2162.
37 V. V. Volkov and K. G. Myakishev, *Inorg. Chim. Acta*, 1999, **289**, 51–57.
38 N. N. Mal'tseva, N. B. Generalova, A. Y. Masanov, K. Y. Zhizhin and N. T. Kuznetsov, *Russ. J. Inorg. Chem.*, 2012, **57**, 1631–1652.
39 V. V. Volkov and K. G. Myakishev, *Radiokhimiya*, 1976, **18**, 512–513.
40 J. Huot, F. Cuevas, S. Deledda, K. Edalati, Y. Filinchuk, T. Grosdidier, C. B. Hauback, M. Heere, R. T. Jensen, M. Latroche and S. Sartori, *Materials*, 2019, **12**, 2778.
41 M. Paskevicius, L. H. Jepsen, P. Schouwink, R. Cerny, D. B. Ravnsbaek, Y. Filinchuk, M. Dornheim, F. Besenbacher and T. R. Jensen, *Chem. Soc. Rev.*, 2017, **46**, 1565–1634.
42 S. R. Daly, D. Y. Kim, Y. Yang, J. R. Abelson and G. S. Girolami, *J. Am. Chem. Soc.*, 2010, **132**, 2106–2107.
43 S. R. Daly, D. Y. Kim and G. S. Girolami, *Inorg. Chem.*, 2012, **51**, 7050–7065.
44 N. R. Rightmire, T. P. Hanusa and A. L. Rheingold, *Organometallics*, 2014, **33**, 5952–5955.
45 D. H. Woen, C. M. Kotyk, T. J. Mueller, J. W. Ziller and W. J. Evans, *Organometallics*, 2017, **36**, 4558–4563.
46 D. H. Woen, J. R. K. White, J. W. Ziller and W. J. Evans, *J. Organomet. Chem.*, 2019, **899**, 120885.
47 T. V. Fetrow, R. Bhowmick, A. J. Achazi, A. V. Blake, F. D. Eckstrom, B. Vlaisavljevich and S. R. Daly, *Inorg. Chem.*, 2020, **59**, 48–61.
48 A. V. Blake, T. V. Fetrow, Z. J. Theiler, B. Vlaisavljevich and S. R. Daly, *Chem. Commun.*, 2018, **54**, 5602–5605.
49 S. R. Daly, P. M. B. Piccoli, A. J. Schultz, T. K. Todorova, L. Gagliardi and G. S. Girolami, *Angew. Chem., Int. Ed.*, 2010, **49**, 3379–3381.
50 S. R. Daly and G. S. Girolami, *Chem. Commun.*, 2010, **46**, 407–408.
51 S. R. Daly and G. S. Girolami, *Inorg. Chem.*, 2010, **49**, 4578–4585.
52 S. R. Daly and G. S. Girolami, *Inorg. Chem.*, 2010, **49**, 5157–5166.
53 S. R. Daly, B. J. Bellott, D. Y. Kim and G. S. Girolami, *J. Am. Chem. Soc.*, 2010, **132**, 7254–7255.
54 N. N. Chang, S. R. Daly and G. S. Girolami, *Polyhedron*, 2019, **162**, 52–58.
55 N. Zohari, R. Fareghi-Alamdari and N. Sheibani, *New J. Chem.*, 2020, **44**, 7436–7449.
56 N. R. Thompson, *J. Chem. Soc.*, 1965, 6290–6295.
57 V. L. Rudzevich, H. Gornitzka, V. D. Romanenko and G. Bertrand, *Chem. Commun.*, 2001, 1634–1635.
58 E. Mayer and A. W. Laubengayer, *Monatsh. Chem.*, 1970, **101**, 1138–1144.
59 E. Mayer and R. E. Hester, *Spectrochim. Acta, Part A*, 1969, **25**, 237–243.
60 E. Mayer, *Angew. Chem., Int. Ed. Engl.*, 1971, **10**, 416–417.

61 P. K. Majhi, A. Koner, G. Schnakenburg, Z. Kelemen, L. Nyulaszi and R. Streubel, *Eur. J. Inorg. Chem.*, 2016, **2016**, 3559–3573.
62 P. C. Keller and L. D. Schwartz, *Inorg. Chem.*, 1971, **10**, 645–647.
63 K. Izod, J. M. Watson, R. W. Harrington and W. Clegg, *Dalton Trans.*, 2021, **50**, 1019–1024.
64 K. Izod, J. M. Watson, W. Clegg and R. W. Harrington, *Inorg. Chem.*, 2013, **52**, 1466–1475.
65 K. Izod, J. M. Watson, W. Clegg and R. W. Harrington, *Dalton Trans.*, 2011, **40**, 11712–11718.
66 T. N. Hooper, M. A. Huertos, T. Jurca, S. D. Pike, A. S. Weller and I. Manners, *Inorg. Chem.*, 2014, **53**, 3716–3729.
67 H. Hofstoetter and E. Mayer, *Monatsh. Chem.*, 1974, **105**, 712–725.
68 H. Hofstoetter and E. Mayer, *Angew. Chem.*, 1973, **85**, 410–411.
69 R. E. Hester and E. Mayer, *Spectrochim. Acta, Part A*, 1967, **23**, 2218–2220.
70 G. S. Girolami, D. Y. Kim, J. R. Abelson, N. Kumar, Y. Yang and S. Daly, Preparation of Metal *N*,*N*-Dimethyldiboranamido Complexes as Precursors for CVD of Metal Containing Films. *US pat.*, 8362220, 2013.
71 J. W. Gilje, K. W. Morse and R. W. Parry, *Inorg. Chem.*, 1967, **6**, 1761–1765.
72 G. Fritz and F. Pfannerer, *Z. Anorg. Allg. Chem.*, 1970, **373**, 30–35.
73 F. Dornhaus, M. Bolte, H.-W. Lerner and M. Wagner, *Eur. J. Inorg. Chem.*, 2006, 1777–1785.
74 J. G. Cordaro, Method for Synthesizing Metal Bis(borano) Hypophosphite Complexes. *US pat.*, 8465715, 2013.
75 L. F. Centofanti, *Inorg. Chem.*, 1973, **12**, 1131–1133.
76 K. X. Bhattacharyya, S. Dreyfuss, N. Saffon-Merceron and N. Mezailles, *Chem. Commun.*, 2016, **52**, 5179–5182.
77 M. R. Anstey, M. T. Corbett, E. H. Majzoub and J. G. Cordaro, *Inorg. Chem.*, 2010, **49**, 8197–8199.
78 L. Maser, K. Flosdorf and R. Langer, *J. Organomet. Chem.*, 2015, **791**, 6–12.
79 L. J. Morris, M. S. Hill, M. F. Mahon, I. Manners and B. O. Patrick, *Organometallics*, 2020, **39**, 4195–4207.
80 F. Dornhaus and M. Bolte, *Acta Crystallogr., Sect. E: Struct. Rep. Online*, 2006, **62**, m3573–m3575.
81 W. Zhang, X. Qi, S. Huang, J. Li, C. Tang, J. Li and Q. Zhang, *J. Mater. Chem. A*, 2016, **4**, 8978–8982.
82 G. A. Bowmaker, *Chem. Commun.*, 2013, **49**, 334–348.
83 T. P. Gompa, N. T. Rice, D. R. Russo, L. M. Aguirre Quintana, B. J. Yik, J. Bacsa and H. S. La Pierre, *Dalton Trans.*, 2019, **48**, 8030–8033.
84 R. Shinomoto, E. Gamp, N. M. Edelstein, D. H. Templeton and A. Zalkin, *Inorg. Chem.*, 1983, **22**, 2351–2355.
85 R. D. Shannon, *Acta Crystallogr., Sect. A*, 1976, **A32**, 751–767.
86 T. J. Marks and J. R. Kolb, *Chem. Rev.*, 1977, **77**, 263–293.
87 S. R. Daly, in *The Heaviest Metals: Science and Technology of the Actinides and Beyond*, ed. W. J. Evans and T. P. Hanusa, 2018, pp. 319-334.
88 H. Braunschweig, A. Gackstatter, T. Kupfer, K. Radacki, S. Franke, K. Meyer, K. Fucke and M. H. Lemee-Cailleau, *Inorg. Chem.*, 2015, **54**, 8022–8028.
89 E. R. Bernstein, W. C. Hamilton, T. A. Keiderling, S. J. La Placa, S. J. Lippard and J. J. Mayerle, *Inorg. Chem.*, 1972, **11**, 3009–3016.
90 E. R. Bernstein, T. A. Keiderling, S. J. Lippard and J. J. Mayerle, *J. Am. Chem. Soc.*, 1972, **94**, 2552–2553.
91 H. I. Schlesinger and H. C. Brown, *J. Am. Chem. Soc.*, 1953, **75**, 219–221.
92 M. N. Bochkarev, *Russ. Chem. Rev.*, 2000, **69**, 783–794.
93 M. N. Bochkarev, *Chem. Rev.*, 2002, **102**, 2089–2117.
94 D. Baudry, E. Bulot and M. Ephritikhine, *J. Chem. Soc., Chem. Commun.*, 1988, 1369–1370.
95 D. Baudry, E. Bulot, P. Charpin, M. Ephritikhine, M. Lance, M. Nierlich and J. Vigner, *J. Organomet. Chem.*, 1989, **371**, 155–162.
96 M. J. Monreal, R. K. Thomson, T. Cantat, N. E. Travia, B. L. Scott and J. L. Kiplinger, *Organometallics*, 2011, **30**, 2031–2038.
97 T. V. Fetrow, J. P. Grabow, J. Leddy and S. R. Daly, *Inorg. Chem.*, 2021, **60**, 7593–7601.
98 G. M. Sheldrick, *Acta Crystallogr., Sect. A: Found. Crystallogr.*, 2008, **64**, 112–122.
99 O. V. Dolomanov, L. J. Bourhis, R. J. Gildea, J. A. K. Howard and H. Puschmann, *J. Appl. Crystallogr.*, 2009, **42**, 339–341.